

Breaking the Encoder Barrier for Seamless Video-Language Understanding

Handong Li^{1,3*} Yiyuan Zhang^{2,4*} Longteng Guo^{1,3*} Xiangyu Yue² Jing Liu^{1,3}

¹School of Artificial Intelligence, University of Chinese Academy of Sciences

²MMLab, CUHK ³Institute of Automation, Chinese Academy of Science ⁴Shanghai AI Lab

Abstract

Most Video-Large Language Models (Video-LLMs) adopt an encoder-decoder framework, where a vision encoder extracts frame-wise features for processing by a language model. However, this approach incurs high computational costs, introduces resolution biases, and struggles to capture fine-grained multimodal interactions. To overcome these limitations, we propose ELVA, an encoder-free Video-LLM that directly models nuanced video-language interactions without relying on a vision encoder. ELVA employs token merging to construct a bottom-up hierarchical representation and incorporates a video guidance supervisor for direct spatiotemporal representation learning. Additionally, a hybrid-resolution mechanism strategically integrates high- and low-resolution frames as inputs to achieve an optimal balance between performance and efficiency. With only 7M publicly available video-text pairs, ELVA achieves performance on par with encoder-based Video-LLMs while reducing FLOPs by up to 95% and inference latency by 92%, offering a scalable and efficient solution for real-time video understanding.

1. Introduction

Building upon the remarkable progress of Large Language Models (LLMs) [2, 32], Video Large Language Models (Video-LLMs) [15, 20, 26] have emerged as a powerful paradigm for video-language understanding. Most existing Video-LLMs follow a modular encoder-decoder architecture, where a pretrained vision encoder (e.g., CLIP [28]) extracts frame-wise visual features, which are then processed by an LLM. While this approach has demonstrated strong performance across various benchmarks, it imposes fundamental limitations that hinder flexibility, efficiency, and scalability—challenges that are particularly pronounced given the complex spatiotemporal nature of video data.

(1) Accumulating Computational Overhead: Unlike

*Equal Contribution.

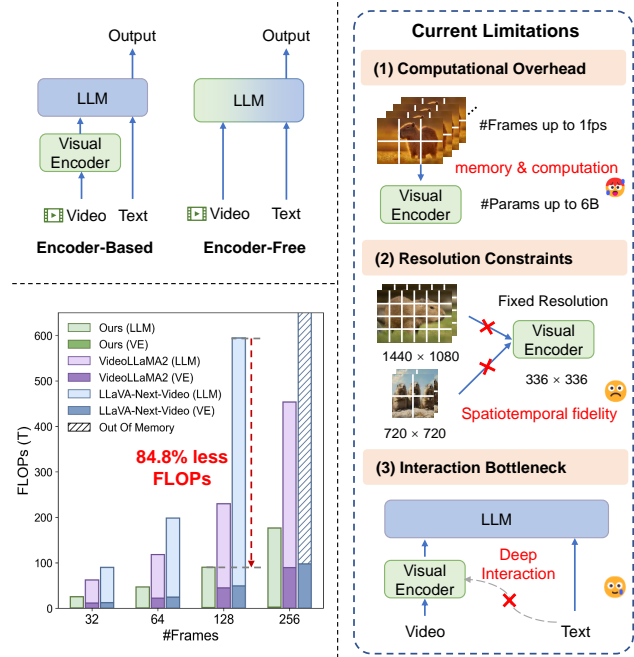


Figure 1. **Encoder-based vs. encoder-free Video-LLMs.** Encoder-based models connect a vision encoder with an LLM, encountering severe issues in effectively handling video data. In contrast, ELVA adopts an encoder-free architecture, directly integrating video perception and language modeling within a unified framework, achieving dramatically higher efficiency.

image models that require only a single forward pass through a vision encoder, video processing scales poorly with sequence length due to frame-wise feature extraction. State-of-the-art vision encoders, often comprising billions of parameters (e.g., InternViT-6B), amplify this issue by demanding prohibitive memory and computation. As a result, extending such models to long or high-resolution videos becomes impractical, limiting real-time applications.

(2) Spatiotemporal Resolution Constraints: Encoder-based models inherently impose resolution biases as they operate on fixed-size visual representations. This compromises spatial and temporal fidelity, particularly in high-resolution, long-duration videos where fine-grained details

are crucial. Moreover, the inability to dynamically adjust resolution based on content restricts adaptability across diverse real-world scenarios.

(3) Multimodal Interaction Bottleneck: Encoder-based approaches primarily rely on pre-extracted features, restricting their ability to capture nuanced, bottom-up interactions between video pixels and text tokens, as well as inter-frame dependencies. This results in suboptimal fusion of multimodal cues, limiting the model’s capacity for holistic video understanding.

To overcome these limitations, we investigate an encoder-free approach that eliminates reliance on pretrained vision encoders, enabling direct video-language modeling. This paradigm shift offers substantial advantages but also presents significant challenges. Ensuring stable training, maintaining competitive performance, and effectively capturing spatiotemporal semantics without explicit feature encoders are non-trivial obstacles. Unlike prior encoder-free models in the image domain (e.g., Fuyu [4], EVE [10]), where vast image datasets facilitate direct pixel-to-token learning, video data introduces additional complexities due to its high dimensionality and temporal dependencies. Despite these challenges, encoder-free Video-LLMs hold great promise for achieving seamless video-language understanding. Yet, their potential remains largely untapped, marking them as a critical frontier in the evolution of Video-LLMs.

In this paper, we introduce **ELVA** (Encoder-free Large Video LAnguage model), a novel Video-LLM that eliminates the reliance on pretrained vision encoders, enabling direct integration of both spatial and temporal information within a unified language modeling framework. By identifying key factors for building efficient Video-LLMs without explicit vision encoders, ELVA offers a more flexible, scalable, and computationally efficient approach to video understanding.

To achieve this, we introduce a native video tokenizer, enabling efficient processing across a wide range of video resolutions and aspect ratios. Then we propose a lightweight video patch embedding layer, which facilitates effective spatiotemporal pre-modeling. To further enhance semantic abstraction within the LLM, hierarchical token merging progressively consolidates low-level tokens into more abstract, higher-level representations. By exploiting redundancy in the video content, this mechanism not only reduces unnecessary complexity but also directs computational resources towards the most salient features. For efficient video representation learning within LLMs, we introduce a video guidance supervisor, wherein a pre-trained video model supervises the learning process through tube-wise and frame-wise loss functions, ensuring the direct learning of spatial-temporal representations from raw pixels. Finally, to optimize inference efficiency, ELVA leverages a hybrid-resolution processing strategy, intelligently

mixing high- and low-resolution frames, thereby balancing computational efficiency with content fidelity.

With 7M publicly available video-text pairs, ELVA surpasses existing encoder-free image counterparts and approaches encoder-based Video-LLMs of similar capacity across diverse vision-language benchmarks. Moreover, ELVA achieves substantial computational gains, reducing FLOPs by 95% and inference latency by 92% compared to typical LLaVA-style baseline [43]. These results establish ELVA as a promising step toward scalable, native, and next-generation Video-LLMs.

Our contribution can be concluded as:

- We propose ELVA, a novel encoder-free Video-LLM that models nuanced video-language interactions in a bottom-up hierarchy, enabling greater flexibility, scalability, and adaptability across diverse video understanding tasks.
- We identify key techniques essential for encoder-free Video-LLMs, including video guidance supervisor for efficient spatiotemporal representation learning within the LLM, and hybrid-resolution inference to enhance inference efficiency and adaptability.
- ELVA demonstrates for the first time that encoder-free Video-LLMs can achieve performance on par with leading encoder-based models while reducing FLOPs by up to 95% and inference latency by 92%. This makes ELVA a highly efficient and practical solution for real-time and long-form video understanding.

2. Related Work

2.1. Video Large Language Models

Video-LLMs process videos by extracting and encoding frames and then rearranging these as final video features. Several works [8, 19] use the Q-Former module from BLIP-2 [9] to merge visual and text features, while others [1, 22, 25, 45] concatenate frame features directly. Video-LLaMA [42] incorporates both visual and auditory content through a Video Q-former for temporal understanding. Video-LLaVA [22] introduced a unified approach that aligns visual representations before projecting them into the language space.

When processing lengthy videos, longer visual tokens need to be properly handled on the LLM side. Video-ChatGPT [26] and PLLaVA [37] employ pooling modules to reduce data dimensions but face challenges regarding computational cost and limitations of the context window. LLaMA-VID [21] employs an additional text decoder to embed the text query for cross-attention between frame features and compress the context token to one token per frame. However, existing work overlooks the increased load on the vision encoder side as the number of frames grows. When processing videos with more than 64 frames (minutes-long video), the latency on the encoder side tends

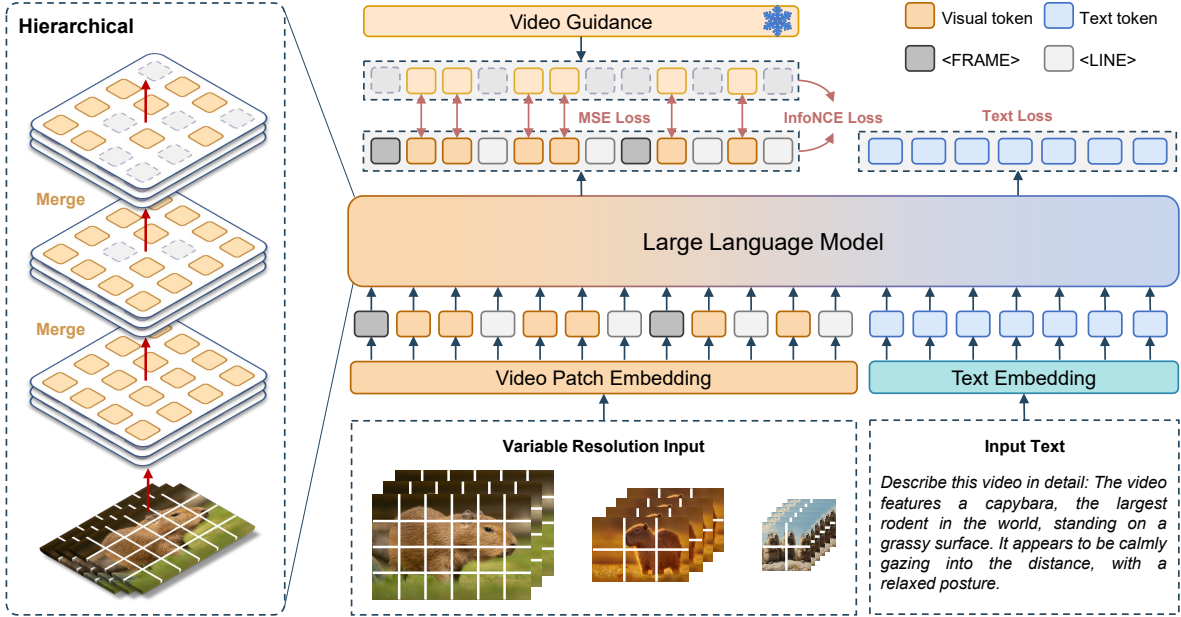


Figure 2. **Framework illustration of ELVA.** ELVA is an encoder-free Video-LLM that captures nuanced video-language interactions through a bottom-up hierarchical design with layer-wise token merging. A video guidance loss enhances spatiotemporal representation learning, while a hybrid-resolution inference strategy optimizes the balance between computational efficiency and content fidelity.

to plateau or even exceed that of the LLM.

2.2. Encoder-Free VLMs

Recently, encoder-free vision-language models have garnered increasing attention, which processes image inputs directly through a decoder-only network. These models can generally be categorized into two types. The first category employs lightweight architectures to obtain continuous visual embeddings of images before feeding them into the LLM. For example, Fuyu-8B [4] processes images directly through a simple linear projection, efficiently handling high-resolution images without relying on a dedicated visual encoder. EVE-7B [10] focuses on vision-language pre-alignment from an LLM-centric perspective, enhancing image recognition through visual representation supervision. SOLO [6] introduces an open-source training framework for developing monolithic multimodal language models (MLLMs). The second category utilizes discrete encoding models to generate visual discrete tokens, such as Chameleon [31], Show-o [35], Transfusion [46], and Emu3 [34]. These models demonstrated the competitive performance of encoder-based VLMs while achieving more efficient computation. However, they predominantly focus on the image modality, with video processing remaining an area in need of further exploration.

3. ELVA

As shown in Figure 2, we first outline the architecture of ELVA, which learns efficient video representation inside the

LLM with just 7 million visual samples.

3.1. Encoder-Free Architecture

Native Video Tokenization. In contrast to conventional approaches, we directly split the original video frames into patches at their native resolution without any preprocessing. To preserve both spatial and temporal information, we introduce special tokens: `<FRAME>` to mark the start of each frame and `<LINE>` to denote the end of a patch’s line in raster-scan order [4]. This approach allows the model to process video inputs with their native resolution and frame length.

Video Patch Embedding Layer. Conventional patch embedding methods often treat visual frames in isolation, neglecting the crucial temporal relationships across frames. This limitation becomes pronounced when comprehending long video sequences. To address this limitation, we propose a computation-efficient video patch embedding layer with a minimal parameter count (9M) that demonstrates effectiveness in spatial-temporal pre-modeling. Specifically, given an input video $x \in \mathbb{R}^{T \times 3 \times H \times W}$, where T denotes the number of frames, and H and W represent the height and width of each frame, respectively. The video is split into patch grids $x \in \mathbb{R}^{T \times \Sigma_i (H_i \cdot W_i / P^2) \times (P^2 \cdot 3)}$, where P is the patch size. For each row of patch grids $\mathbb{R}^{T \times \Sigma_i (W_i / P) \times (P^2 \cdot 3)}$, we add a learnable token `<LINE>` to introduce spatial modeling. Similarly, the patch grids of a frame are added `<FRAME>` learnable tokens to introduce temporal modeling. Then, we project patch grids to

video embeddings $x \in \mathbb{R}^{T \times \Sigma_i(H_i \cdot W_i / P^2) \times D}$, where D is the embedding dimension. And video embeddings construct long-range spatial-temporal relationships by a cross-attention layer: we use `<FRAME>` token to query the video embeddings of a frame and use `<LINE>` token to query video embeddings in each row.

Hierarchical Merging. To address spatiotemporal redundancy and enhance semantic abstraction, we introduce a hierarchical merging mechanism that efficiently consolidates video tokens, minimizing unnecessary complexity and focusing computational resources on the most salient video features. Different from previous methods [37, 44] using pooling or slow-fast [16] to compress video tokens, we progressively compares the similarity between neighborhood video tokens, then drops and merges redundant tokens on the temporal dimension across different LLM layers. Specifically, for l -th layer, video tokens denoted by $f^l \in \mathbb{R}^{N_l \times D}$. In the hierarchical merging process, we maintain an index matrix M of a certain shape $T \times (H \cdot W / P^2)$. For example, M_{ij}^l denotes the index of l -th layer on the i -th frame and j -th video token. In the hierarchical process, the index matrix in the l -th layer is updated as:

$$s_{ij} = \langle f_{ij}^l, f_{(i+1)j}^l \rangle, \quad M_{ij}^l = \begin{cases} 1, & s_{ij} \leq \tau \\ 0, & s_{ij} > \tau \end{cases}, \quad (1)$$

where $\langle \cdot, \cdot \rangle$ is the cosine similarity, and τ is the threshold, set to 0.6. Then, we merge the redundant tokens by meaning. After hierarchical merging, the input of the $l+1$ -th layer is $f^{l+1} \in \mathbb{R}^{N_{l+1} \times D}$, where $N_{l+1} = \sum_i \sum_j M_{ij}^l$. For different depths, hierarchical merging follows a different policy: in the shallow layers, patches with similarity above a predefined threshold are merged, while in the deep layers, merging continues until a target compression ratio (detailed in 3, 50% in our experiment) is reached. This approach effectively enhances computational efficiency while preserving crucial visual information in the encoder-free framework.

3.2. Video Guidance Supervisor

To directly model spatiotemporal interactions without relying on a vision encoder, we introduce a video guidance supervisor that steers the learning process towards effective video representation. Specifically, we use the pretrained SigLIP [40] model as a teacher, and design two complementary loss functions at the tube-wise and frame-wise levels. These losses guide the model to learn rich temporal semantics from raw pixel data, without requiring an explicit vision encoder. By integrating these losses with the language-centric generative loss, the model can capture both spatial and temporal information effectively. Experiments in Sec 4.2 show that the three losses work synergistically, offering complementary benefits.

Tube-Wise Visual Alignment Loss. To capture temporal dynamics at the tube level, we employ the guidance model to align temporal features. We compute a mean squared error (MSE) loss between the LLM’s visual features (\mathbf{f}_{vis}) from its final layer and the video encoder’s penultimate layer features ($\mathbf{f}_{\text{target}}$). Both features are reshaped to maintain the original aspect ratio, with adaptive pooling applied for resolution alignment when necessary. Tube-level semantics are captured through mean pooling across frames, followed by MSE-based feature alignment (\mathcal{L}_{MSE}) between normalized \mathbf{f}_{vis} and $\mathbf{f}_{\text{target}}$.

$$\mathcal{L}_{\text{MSE}} = \text{MSE} \left(\frac{\mathbf{f}_{\text{vis}}}{\|\mathbf{f}_{\text{vis}}\|_2}, \frac{\mathbf{f}_{\text{target}}}{\|\mathbf{f}_{\text{target}}\|_2} \right) \quad (2)$$

Frame-Wise Visual Contrastive Loss. To improve global information perception, we employ contrastive loss (\mathcal{L}_{Con}). The `<FRAME>` token is preserved from the LLM’s final layer visual tokens, while maintaining the target features. For each feature pair ($\mathbf{f}_{\text{vis}}, \mathbf{f}_{\text{target}}$), we perform frame-wise mean pooling and batch-dimension reshaping. \mathcal{L}_{Con} is computed using normalized features aggregated across all GPUs. The contrastive loss is defined as follows, where $\mathbf{f}_{\text{target}}$, B and τ represent the batch size and a learnable parameter, respectively.

$$\mathcal{L}_{\text{Con}} = -\frac{1}{2} \sum_{i=1}^B \log \frac{\exp(\tau \cdot (\mathbf{f}_{\text{vis},i}^\top \mathbf{f}_{\text{target},i}))}{\sum_{j=1}^B \exp(\tau \cdot (\mathbf{f}_{\text{vis},i}^\top \mathbf{f}_{\text{target},j}))} - \frac{1}{2} \sum_{i=1}^B \log \frac{\exp(\tau \cdot (\mathbf{f}_{\text{vis},i}^\top \mathbf{f}_{\text{target},i}))}{\sum_{j=1}^B \exp(\tau \cdot (\mathbf{f}_{\text{vis},j}^\top \mathbf{f}_{\text{target},i}))} \quad (3)$$

With the generative visual caption loss \mathcal{L}_{Gen} , the overall training loss is formulated as:

$$L = L_{\text{Gen}} + L_{\text{MSE}} + L_{\text{Con}} \quad (4)$$

These two learning objectives, spanning different levels, can effectively help the encoder-free model rapidly acquire valuable visual knowledge from both the training data and the guidance model—an outcome that cannot be achieved by relying solely on the generative visual caption loss \mathcal{L}_{Gen} .

3.3. Training Procedure

Video Recaption Pretraining Data. The quality of visual captions used during pretraining significantly impacts Video-LLM performance, with poor caption quality often leading to decreased generalization and diminished language logic abilities after the full fine-tuning of the LLM. Open-source models now available can generate high-quality descriptions for both images and videos, with customizable prompts that incorporate grounding information,

OCR details, and domain-specific knowledge. This capability inspired us to reprocess open-access data into dense, high-quality, and detailed captions. By leveraging Qwen2-VL [33], we enable the effective utilization of large-scale image and video data in the LLM era, with content description prompts for images that emphasize world knowledge, detection, and OCR, while utilizing video prompts that emphasize temporal event sequencing. Further details of the recaption process can be found in the Appendix A.1.

Directly perceiving videos poses a substantial challenge for encoder-free models. To fully learn spatiotemporal representation inside the LLM, we propose a progressive training paradigm with 3 stages.

Stage1. Spatial Pretraining. To accommodate the new modality and address the challenges of training an encoder-free model, we initiate a warm-up phase to pre-adapt the LLM to pixel inputs. During this phase, we treat images as single-frame videos and train the model exclusively on ELVA-Image. Leveraging our high-quality re-annotated dense captions, we aim to enable the model to learn fundamental visual information, such as entity attributes and spatial locations, directly from raw pixel inputs. Images with varying aspect ratios encourage the model to learn the spatial relationships between patch rows, thereby enabling support for arbitrary resolutions.

Stage2. Spatial-Temporal Pretraining. In this stage, we incorporate the remaining 3M ELVA-Video samples into the model. By preserving the original aspect ratio, videos are processed into dynamic frames to capture temporal relationships. As in the Visual Warm-up phase, all three loss functions are simultaneously applied to guide the model at multiple levels. With temporal guidance provided by the video encoder and our re-annotated video captions, the model efficiently learns spatiotemporal representations, thereby establishing a robust foundation for the subsequent training phase.

Stage3. Supervised Fine-tuning (SFT). To focus on developing a visually-oriented language capability, this stage exclusively utilizes the text generative loss. We employ both image and video Supervised Fine-Tuning (SFT) data simultaneously to enable multimodal capabilities. The dataset encompasses a diverse range of text formats, including visual descriptions, question-answering, reasoning, multiple-choice, and others, to more effectively transfer the pretraining knowledge acquired in earlier stages to the model’s conversational abilities.

3.4. Hybrid Resolution Inference

Unlike encoder-based models, ELVA can efficiently handle visual sequences across different input resolutions.

This capability is made possible by the use of special tokens `<FRAME>` and `<LINE>`, which allow the model to maintain consistency in visual sequence representation regardless of the resolution and frame number. One of the key advantages of ELVA’s approach is its ability to simultaneously support high-resolution and low-resolution frames within a single video. For long videos, the model can selectively process some high-resolution frames while using low-resolution frames for others, thus significantly reducing computational load without compromising performance, detailed in Section 4.2. This hybrid resolution strategy ensures that the model remains computationally efficient without sacrificing the quality of visual information.

4. Experiment

In this section, we present the experimental setup, details of the datasets, and comparisons with state-of-the-art methods across multiple video benchmarks. Additional details are provided in the Appendix.

Implementation Details. We implement our ELVA model using the Qwen2-1.5B and Qwen2-7B backbones to accommodate different model sizes. To enhance efficiency, we constrain the longest edge of each image (frame) to a fixed length of 448 pixels during the early alignment stages and 672 pixels during the supervised fine-tuning (SFT) stage while preserving the original aspect ratio. Following the EVE approach, we introduce a high-resolution training strategy exclusively during the SFT stage to develop the ELVA-7B (HD) model, where the longest image edge is set to 1,344 pixels. The batch sizes for each training stage are 256, 256, and 128, respectively, with the entire training process taking approximately 7 days on 32 NVIDIA A100 GPUs. For hierarchical merging, we set the similarity threshold to 0.6 and apply a compression ratio of 50%. During inference, the hybrid resolution strategy defaults to using 32 high-resolution frames and 32 low-resolution frames, where the longest edge of the low-resolution frames is set to 336.

Training Data. During the three-stage training process, we utilize 4M samples from ELVA-Image, 3M samples from ELVA-Video, and a supervised fine-tuning (SFT) dataset comprising 665K image samples and 178K video samples. An additional 3M image SFT samples are used while training the HD model. Specifically, ELVA-Image consists of 1M original samples from DenseFusion and 3M re-annotated samples from the CC3M and COCO datasets. ELVA-Video includes 2M samples from WebVid [3] and 1M samples from VALOR [5]; all captions are re-annotated. Further details of the implementation can be found in the Appendix A.1.

Table 1. **Performance on zero-shot video-language benchmarks.** We evaluate ELVA on 3 short-video benchmarks and 5 long-video benchmarks. VC denotes Video-ChatGPT. The results in **bold** and underline values indicate the best and second-best performance among encoder-free models, respectively. * indicates that the result is evaluated by us.

Model	LLM Size	Short Video benchmark			Long Video benchmark				
		MSVD	ActivityNet	VC	EgoSchema	MVBench	VideoMME	MLVU	CinePile
<i>Proprietary Models</i>									
Gemini 1.0 Pro	-	-	49.8 / -	-	55.7	-	-	-	-
GPT-4V	-	-	59.5 / -	4.06	55.6	43.7	59.9	-	58.8
Pegasus-1	-	-	59.9 / -	3.84	-	-	-	-	-
<i>Encoder-based Models</i>									
VideoLLaMA [41]	7B	51.6 / 2.5	12.4 / 1.1	1.98	-	34.1	-	-	-
VideoChat [18]	7B	56.3 / 2.8	26.5 / 2.2	2.29	-	35.5	-	-	-
Video-ChatGPT [26]	7B	64.9 / 3.3	35.2 / 2.7	2.42	-	32.7	-	31.3	14.6
Chat-UniVi [15]	7B	65.0 / 3.6	46.1 / 3.3	2.99	-	-	-	-	-
Video-LLaVA [22]	7B	70.7 / 3.9	45.3 / 3.3	2.84	38.4	41.0	39.9	47.3	22.5
LLAMA-VID [21]	7B	69.7 / 3.7	47.4 / 3.3	2.89	38.5	41.9	25.9	33.2	-
LLaVA-NeXT-Video [23]	7B	67.8 / 3.5	53.5 / 3.2	3.26	43.9	33.7	46.5	-	-
VideoChat2 [19]	7B	70.0 / 3.9	49.1 / 3.3	2.95	54.4	60.4	42.3	47.9	29.3
VideoLLaMA2 [8]	7B	70.9 / 3.8	50.2 / 3.3	3.13	51.7	54.6	46.6	48.5	44.6
<i>Encoder-Free Models</i>									
Fuyu* [4]	8B	56.8 / 3.5	28.8 / 2.6	1.90	20.6	31.6	28.7	31.1	26.0
EVE* [10]	7B	<u>61.4 / 3.6</u>	41.8 / 3.3	2.16	38.2	34.9	29.3	36.8	26.4
ELVA	1.5B	60.1 / 3.6	<u>44.6 / 3.3</u>	<u>2.63</u>	<u>40.8</u>	<u>43.5</u>	<u>41.8</u>	<u>47.6</u>	<u>41.2</u>
ELVA	7B	65.2 / 3.7	48.7 / 3.5	2.73	48.3	51.2	47.1	51.8	46.1

4.1. Main Results

We evaluate ELVA on a series of comprehensive visual-language benchmarks: **1)** Video-based benchmarks include MSVD-QA [36], ActivityNet-QA [39], Video generative benchmark [26] and **2)** Long Video Understanding encompass Egoschema [27], CinePile [29], VideoMME [13], MVBench [19], MLVU [47]. The video performance of encoder-free models is evaluated by us. Due to limitations in these models’ original context lengths, which cannot support more than 4 frames, we maintain a total visual token length of approximately 8192 and apply RoPE scaling to extend their positional encoding length.

We evaluate ELVA’s video capabilities across three short video tasks and five long video tasks. In Table 1, we observe that our 1.5B model achieves a competitive result in MSVD and ActivityNet with several 7B encoder-based models like Chat-UniV and Video-LLaVA. Furthermore, ELVA (7B) significantly outperforms most existing encoder-based video-language models, approaching state-of-the-art performance especially on long video benchmarks. This underscores ELVA’s exceptional video comprehension abilities and its scalable capability. Our model also surpasses existing encoder-free models by a substantial margin. We also observe that EVE, despite being pre-trained solely on images, demonstrates strong performance on short-video tasks but struggles with long-video tasks. This suggests that short-video benchmarks primarily require spatial modeling. Our tow stage pretraining further prove this. As shown in the figure 4, MSVD performance

improves more rapidly during Stage 1, while VideoMME exhibits significant gains only in Stage 2. This is because short-video QA tasks mainly focus on entity attributes and action categories, whereas long-video QA involves more complex challenges such as scene changes and event reasoning, which further underscores the importance of our two-stage pretraining strategy.

4.2. Ablation Study

For the default settings in ablation studies, we use our 7B model with all parameters kept tuned. To reduce computational costs, only the MSE loss and generative loss are applied. Additionally, a randomly selected subset of 1M samples from the full 7M dataset is used.

Effect of Video Patch Embedding Layer. To assess the effect of the lightweight video patch embedding on the overall model, we trained two models: one with only a naive patch embedding layer and another with the additional cross attention block we used. The experiments in Table 3 reveal that the block improves performance for both short and long video tasks, with a particularly significant enhancement in long video tasks, yielding an average improvement of 2.53%. This indicates that our lightweight video patch embedding block effectively captures temporal features, contributing to the model’s ability to represent long sequences.

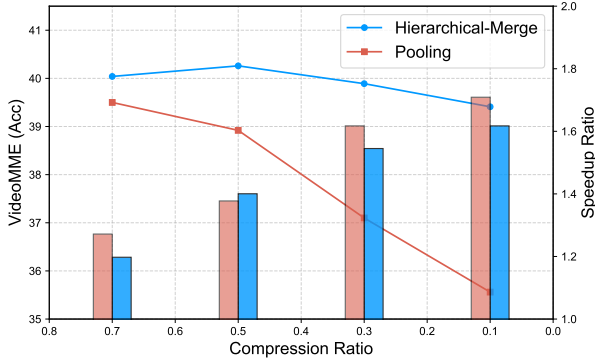


Figure 3. **The effect of hierarchical merging on accuracy and inference speedup across layer compression ratios.** VideoMME (Acc) is presented using a line chart, while the speedup ratio is illustrated with a bar chart.

Table 2. **Ablation study on pre-training data type, data scale, and objective.**

Model	Factors	GQA	SEED-I	MSVD	VideoMME
Pre-training Data Type					
(a)	Original Image+Video	42.1	42.1	46.0	34.2
(b)	Recap Image	44.9	46.6	47.2	37.6
(c)	Recap Video	44.2	41.4	47.0	37.9
(d)	Recap Image+Video	46.1	45.9	49.4	38.5
Pre-training Data Scale					
(e)	1M	43.6	42.6	47.1	38.1
(f)	3M	45.4	47.2	48.8	37.4
(g)	7M	46.1	45.9	49.4	38.5
Pre-Training Objective					
(h)	\mathcal{L}_{Gen}	42.2	40.0	45.8	37.9
(i)	$\mathcal{L}_{Gen} + \mathcal{L}_{MSE}$	43.6	42.6	47.1	38.1
(j)	$\mathcal{L}_{Gen} + \mathcal{L}_{Con}$	42.4	41.0	47.4	38.5
(k)	$\mathcal{L}_{Gen} + \mathcal{L}_{MSE} + \mathcal{L}_{Con}$	44.4	44.8	48.0	38.5

Effect of Hierarchical Merge. With 32 frames fixed at a maximum edge length of 672 pixels, we evaluate the ST-Merge method under different compression ratios. We compare our approach with a pooling method that is directly applied after the patch embedding layer. As shown in Figure 3, as the token compression ratio increases, the pooling method results in a substantial decrease in long-video performance, whereas ST-Merge maintains performance and only exhibits a slight degradation beyond a certain compression threshold. This demonstrates that directly applying pooling before the LLM in encoder-free models compromises spatiotemporal representations, further underscoring the advantages of our hierarchical compression strategy.

Video Guidance v.s. Image Guidance. We observe that when utilizing features from different Vision Transformer (ViT) encoders as training targets, those pre-trained in video data significantly enhance the model’s understanding of visual tasks. In particular, we use EVA-CLIP-g and Siglipso-400M [40] as different encoder backbones, along with their video-pretrained counterparts (which are trained using InfoNCE loss with BERT on a dataset of 10M video

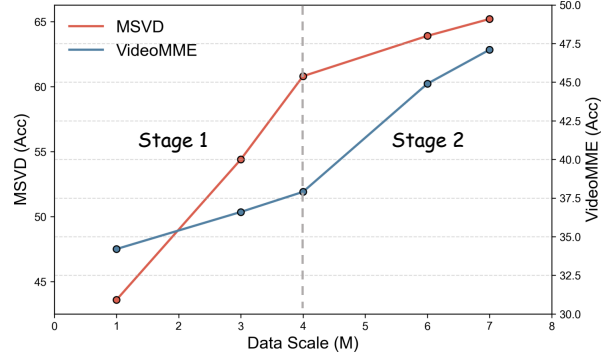


Figure 4. **Effect of pre-training data size across two pre-training stages.** All checkpoint results are reported after undergoing the same instruction tuning process.

Table 3. **Effect of Video Patch Embedding Layer.** Naive PEL, Video PEL represent the patch embedding layer used commonly in CLIP and our spatial-temporal patch embedding layer respectively.

Arch	Cross-attn	Params.	MSVD	VideoMME
Naive PEL	✗	6M	48.7	39.6
Video PEL	✓	9M	49.9	42.2

clips, including WebVid [3] and HDVILA [38]). As shown in Table 4, across short video and long video benchmarks, the visual features derived from pretrained video encoders improve performance by an average of approximately one point per task.

Caption Data Quality. From (a) to (d) in Table 2, we use the original captions from the 7M pretraining dataset as the baseline and train models separately on Recap Image (ELVA-Image), Recap Video (ELVA-Video), and Recap Image+Video to evaluate the impact of recapition quality. As shown in the table, Recap Image outperforms the baseline on vision benchmarks (GQA, SEED-I), while Recap Video achieves comparable performance on image tasks and excels in video-related tasks (MSVD, VideoMME). The full Recap dataset leads to a substantial performance boost, with improvements of 4.0% on GQA, 3.8% on SEED-I, 3.4% on MSVD, and 4.3% on VideoMME. This demonstrates that original captions degrade performance, highlighting the importance of recapition. Additionally, we randomly select 1M and 3M subsets from the 7M dataset to examine the effect of data scale. From (e) to (g), increasing the dataset size further enhances performance, particularly in general vision and short-video tasks.

Pretraining Objectives. From (h) to (k), we analyze the impact of each pretraining objective. We use generative loss as the baseline to assess the influence of other pretraining objectives. It can be observed that the join of MSE loss

Table 4. **Effect of using different vision encoders for feature distillation.** Video Pretrained indicates the encoder is pre-training on an additional 10M video clips [38].

Encoder	Video Pretrained	MSVD-QA	VideoMME
EVA_CLIP-g [30]	✗	46.1	36.8
	✓	47.1	38.4
Siglip-so-400M [40]	✗	47.4	41.0
	✓	49.9	42.2

Table 5. **Inference speed comparison of ELVA and LLaVA-Next-Video.** ‘Merge’ denotes hierarchical token merging and ‘HR’ denotes hybrid resolution inference. MEM, FLOPs, and TTFT denote max memory allocated, floating point operations per second, and the time to first token in seconds, respectively.

#Frames	Model	MEM (G)	FLOPs (T)	TTFT (s)
32	Encoder-based	20.7	260	2.59
	Encoder-free	20.0 (-3%)	75 (-71%)	0.51 (-80%)
	+ Merge	16.4 (-21%)	25 (-90%)	0.26 (-90%)
	+ Merge + HR	15.5 (-25%)	14 (-95%)	0.22 (-92%)
64	Encoder-based	27.6	517	5.92
	Encoder-free	25.4 (-8%)	146 (-72%)	1.11 (-81%)
	+ Merge	18.0 (-35%)	47 (-91%)	0.46 (-92%)
	+ Merge + HR	16.3 (-41%)	24 (-95%)	0.27 (-95%)
128	Encoder-based	41.4	1030	15.18
	Encoder-free	39.6 (-4%)	289 (-72%)	2.14 (-86%)
	+ Merge	22.5 (-46%)	104 (-90%)	0.97 (-94%)
	+ Merge + HR	18.5 (-55%)	44 (-96%)	0.56 (-96%)

enhances general visual capabilities, while contrastive loss contributes to improved more video understanding. The combination of generative losses, MSE loss, and contrastive loss ($\mathcal{L}_{\text{Gen}} + \mathcal{L}_{\text{MSE}} + \mathcal{L}_{\text{Con}}$) yields the best overall performance, demonstrating the value of integrating multiple complementary objectives.

4.3. Inference Efficiency

Comparison with Encoder-Based Model. In Table 5, we compare the inference efficiency of our encoder-free model with encoder-based models across different frame counts. For encoder-based model, we directly concat video tokens with text tokens. Models are deployed on an NVIDIA A100, with the number of output tokens fixed as 120. Without any processing, directly inputting video pixels leads to higher peak memory usage and FLOPs for the encoder-free model. However, despite this, our model still achieves a 80% advantage in TTFT (Time to First Token), benefiting from the ultra-low latency enabled by bypassing explicit frame encoding.

When applying the ST-Merge method, our model reduces token length by nearly 50% without significant performance degradation. Additionally, incorporating hybrid resolution during inference further enhances efficiency and long-video performance. As a result, our model scales more effectively with increasing frame counts. Notably, at 128

Table 6. **Mixture of Resolutions while Inference.** We evaluate the models on 2 long video benchmarks under varying video frames.

#Frames		#Input Tokens	VideoMME	MLVU
High-Res	Low-Res			
8	16	5976	42.9	44.1
8	32	7144	43.0	45.2
16	0	9616	37.1	42.2
16	8	10200	42.6	43.5
16	16	10784	43.0	45.4
32	0	19232	42.7	43.8

frames, our TTFT is only 0.56, making it 96% faster than the encoder-based counterpart.

Effect of Hybrid Resolution Inference. To fully validate the hybrid resolution inference approach, we experimented with various combinations of high-resolution and low-resolution frames on our 1.5B model while disabling the spatial-temporal merge strategy. In this setup, the large frames maintained a maximum edge length of 672 pixels, while the small frames were constrained to 224 pixels. For a more effective comparison, we provide the total visual token length for each group, which is directly related to visual information and the model’s computational complexity.

As demonstrated in Table 6, increasing the number of low-resolution frames while keeping the number of high-resolution frames fixed significantly enhances the model’s capability to process long videos, resulting in a 5.9% performance improvement on the VideoMME and 3.2% MLVU benchmarks. Furthermore, with an equivalent frame number, hybrid resolution outperforms high-res with a half token length. This further underscores the superiority of our approach in the long video domain, as it allows for flexible combinations at the input stage to benefit from a greater number of frames.

5. Conclusion

We introduce ELVA, an encoder-free Video-LLM that models video-language interactions without relying on pretrained vision encoders. By leveraging a bottom-up hierarchical merging strategy, video-centric teacher-guided learning, and a hybrid-resolution mechanism, ELVA achieves performance comparable to encoder-based Video-LLMs while significantly enhancing computational efficiency, reducing FLOPs by 95% and inference latency by 92%. Our findings highlight the feasibility of encoder-free Video-LLMs, providing insights into key architectural and training strategies for nuanced video-language modeling directly from raw video data. These results position ELVA as a promising step toward scalable, native, and next-generation Video-LLMs.

References

- [1] Kirolos Ataallah, Xiaoqian Shen, Eslam Abdelrahman, Essam Sleiman, Deyao Zhu, Jian Ding, and Mohamed Elhoseiny. Minigt4-video: Advancing multimodal llms for video understanding with interleaved visual-textual tokens. *arXiv preprint arXiv:2404.03413*, 2024. 2
- [2] Jinze Bai, Shuai Bai, Shusheng Yang, Shijie Wang, Sinan Tan, Peng Wang, Junyang Lin, Chang Zhou, and Jingren Zhou. Qwen-vl: A frontier large vision-language model with versatile abilities. *arXiv preprint arXiv:2308.12966*, 2023. 1, 11
- [3] Max Bain, Arsha Nagrani, Gül Varol, and Andrew Zisserman. Frozen in time: A joint video and image encoder for end-to-end retrieval. In *ICCV*, pages 1728–1738, 2021. 5, 7, 11
- [4] Rohan Bavishi, Erich Elsen, Curtis Hawthorne, Maxwell Nye, Augustus Odena, Arushi Somani, and Saġnak Taşirlar. Introducing our multimodal models, 2023. 2, 3, 6, 11
- [5] Sihan Chen, Xingjian He, Longteng Guo, Xinxin Zhu, Weining Wang, Jinhui Tang, and Jing Liu. Valor: Vision-audio-language omni-perception pretraining model and dataset. *arXiv preprint arXiv:2304.08345*, 2023. 5, 11
- [6] Yangyi Chen, Xingyao Wang, Hao Peng, and Heng Ji. A single transformer for scalable vision-language modeling. *arXiv preprint arXiv:2407.06438*, 2024. 3
- [7] Yangyi Chen, Xingyao Wang, Hao Peng, and Heng Ji. Solo: A single transformer for scalable vision-language modeling, 2024. 11
- [8] Zesen Cheng, Sicong Leng, Hang Zhang, Yifei Xin, Xin Li, Guanzheng Chen, Yongxin Zhu, Wenqi Zhang, Ziyang Luo, Deli Zhao, et al. Videollama 2: Advancing spatial-temporal modeling and audio understanding in video-llms. *arXiv preprint arXiv:2406.07476*, 2024. 2, 6
- [9] Wenliang Dai, Junnan Li, Dongxu Li, Anthony Meng Huat Tiong, Junqi Zhao, Weisheng Wang, Boyang Li, Pascale Fung, and Steven Hoi. Instructblip: Towards general-purpose vision-language models with instruction tuning, 2023. 2
- [10] Haiwen Diao, Yufeng Cui, Xiaotong Li, Yuezhe Wang, Huchuan Lu, and Xinlong Wang. Unveiling encoder-free vision-language models. *arXiv preprint arXiv:2406.11832*, 2024. 2, 3, 6, 11
- [11] Haodong Duan, Junming Yang, Yuxuan Qiao, Xinyu Fang, Lin Chen, Yuan Liu, Xiaoyi Dong, Yuhang Zang, Pan Zhang, Jiaqi Wang, et al. Vlmevalkit: An open-source toolkit for evaluating large multi-modality models. In *Proceedings of the 32nd ACM International Conference on Multimedia*, pages 11198–11201, 2024. 11
- [12] Chaoyou Fu, Peixian Chen, Yunhang Shen, Yulei Qin, Mengdan Zhang, Xu Lin, Zhenyu Qiu, Wei Lin, Jinrui Yang, Xiawu Zheng, et al. Mme: A comprehensive evaluation benchmark for multimodal large language models. *arXiv preprint arXiv:2306.13394*, 2023. 11
- [13] Chaoyou Fu, Yuhan Dai, Yongdong Luo, Lei Li, Shuhuai Ren, Renrui Zhang, Zihan Wang, Chenyu Zhou, Yunhang Shen, Mengdan Zhang, et al. Video-mme: The first-ever comprehensive evaluation benchmark of multi-modal llms in video analysis. *arXiv preprint arXiv:2405.21075*, 2024. 6
- [14] Drew A Hudson and Christopher D Manning. Gqa: A new dataset for real-world visual reasoning and compositional question answering. In *CVPR*, 2019. 11
- [15] Peng Jin, Ryuichi Takano, Wancai Zhang, Xiaochun Cao, and Li Yuan. Chat-univi: Unified visual representation empowers large language models with image and video understanding. In *Proceedings of the IEEE/CVF Conference on Computer Vision and Pattern Recognition*, pages 13700–13710, 2024. 1, 6
- [16] Evangelos Kazakos, Arsha Nagrani, Andrew Zisserman, and Dima Damen. Slow-fast auditory streams for audio recognition. In *ICASSP 2021-2021 IEEE International Conference on Acoustics, Speech and Signal Processing (ICASSP)*, pages 855–859. IEEE, 2021. 4
- [17] Bohao Li, Rui Wang, Guangzhi Wang, Yuying Ge, Yixiao Ge, and Ying Shan. Seed-bench: Benchmarking multimodal llms with generative comprehension. *arXiv preprint arXiv:2307.16125*, 2023. 11
- [18] KunChang Li, Yanan He, Yi Wang, Yizhuo Li, Wenhui Wang, Ping Luo, Yali Wang, Limin Wang, and Yu Qiao. Videochat: Chat-centric video understanding. *arXiv preprint arXiv:2305.06355*, 2023. 6
- [19] Kunchang Li, Yali Wang, Yanan He, Yizhuo Li, Yi Wang, Yi Liu, Zun Wang, Jilan Xu, Guo Chen, Ping Luo, et al. Mvbench: A comprehensive multi-modal video understanding benchmark. In *Proceedings of the IEEE/CVF Conference on Computer Vision and Pattern Recognition*, pages 22195–22206, 2024. 2, 6
- [20] Yanwei Li, Chengyao Wang, and Jiaya Jia. Llama-vid: An image is worth 2 tokens in large language models. *arXiv preprint arXiv:2311.17043*, 2023. 1
- [21] Yanwei Li, Chengyao Wang, and Jiaya Jia. Llama-vid: An image is worth 2 tokens in large language models. In *European Conference on Computer Vision*, pages 323–340. Springer, 2025. 2, 6
- [22] Bin Lin, Yang Ye, Bin Zhu, Jiayi Cui, Munan Ning, Peng Jin, and Li Yuan. Video-llava: Learning united visual representation by alignment before projection. *arXiv preprint arXiv:2311.10122*, 2023. 2, 6
- [23] Haotian Liu, Chunyuan Li, Yuheng Li, and Yong Jae Lee. Improved baselines with visual instruction tuning, 2023. 6, 11
- [24] Yuan Liu, Haodong Duan, Yuanhan Zhang, Bo Li, Songyang Zhang, Wangbo Zhao, Yike Yuan, Jiaqi Wang, Conghui He, Ziwei Liu, et al. Mmbench: Is your multi-modal model an all-around player? *arXiv preprint arXiv:2307.06281*, 2023. 11
- [25] Ruipu Luo, Ziwang Zhao, Min Yang, Junwei Dong, Da Li, Pengcheng Lu, Tao Wang, Linmei Hu, Minghui Qiu, and Zhongyu Wei. Valley: Video assistant with large language model enhanced ability. *arXiv preprint arXiv:2306.07207*, 2023. 2
- [26] Muhammad Maaz, Hanoona Rasheed, Salman Khan, and Fahad Shahbaz Khan. Video-chatgpt: Towards detailed video understanding via large vision and language models. *arXiv preprint arXiv:2306.05424*, 2023. 1, 2, 6

- [27] Karttikeya Mangalam, Raiymbek Akshulakov, and Jitendra Malik. Egoschema: A diagnostic benchmark for very long-form video language understanding. *Advances in Neural Information Processing Systems*, 36:46212–46244, 2023. 6
- [28] Alec Radford, Jong Wook Kim, Chris Hallacy, Aditya Ramesh, Gabriel Goh, Sandhini Agarwal, Girish Sastry, Amanda Askell, Pamela Mishkin, Jack Clark, et al. Learning transferable visual models from natural language supervision. In *ICML*, pages 8748–8763. PMLR, 2021. 1
- [29] Ruchit Rawal, Khalid Saifullah, Miquel Farré, Ronen Basri, David Jacobs, Gowthami Somepalli, and Tom Goldstein. Cinepile: A long video question answering dataset and benchmark. *arXiv preprint arXiv:2405.08813*, 2024. 6
- [30] Quan Sun, Yuxin Fang, Ledell Wu, Xinlong Wang, and Yue Cao. Eva-clip: Improved training techniques for clip at scale. *arXiv preprint arXiv:2303.15389*, 2023. 8
- [31] Chameleon Team. Chameleon: Mixed-modal early-fusion foundation models. *arXiv preprint arXiv:2405.09818*, 2024. 3, 11
- [32] Hugo Touvron, Thibaut Lavril, Gautier Izacard, Xavier Martinet, Marie-Anne Lachaux, Timothée Lacroix, Baptiste Rozière, Naman Goyal, Eric Hambro, Faisal Azhar, et al. Llama: Open and efficient foundation language models. *arXiv preprint arXiv:2302.13971*, 2023. 1
- [33] Peng Wang, Shuai Bai, Sinan Tan, Shijie Wang, Zhihao Fan, Jinze Bai, Keqin Chen, Xuejing Liu, Jialin Wang, Wenbin Ge, Yang Fan, Kai Dang, Mengfei Du, Xuancheng Ren, Rui Men, Dayiheng Liu, Chang Zhou, Jingren Zhou, and Junyang Lin. Qwen2-vl: Enhancing vision-language model’s perception of the world at any resolution. *arXiv preprint arXiv:2409.12191*, 2024. 5, 11
- [34] Xinlong Wang, Xiaosong Zhang, Zhengxiong Luo, Quan Sun, Yufeng Cui, Jinsheng Wang, Fan Zhang, Yueze Wang, Zhen Li, Qiyang Yu, et al. Emu3: Next-token prediction is all you need. *arXiv preprint arXiv:2409.18869*, 2024. 3
- [35] Jinheng Xie, Weijia Mao, Zechen Bai, David Junhao Zhang, Weihao Wang, Kevin Qinghong Lin, Yuchao Gu, Zhijie Chen, Zhenheng Yang, and Mike Zheng Shou. Show-o: One single transformer to unify multimodal understanding and generation. *arXiv preprint arXiv:2408.12528*, 2024. 3
- [36] Dejing Xu, Zhou Zhao, Jun Xiao, Fei Wu, Hanwang Zhang, Xiangnan He, and Yueting Zhuang. Video question answering via gradually refined attention over appearance and motion. In *ACM Multimedia*, 2017. 6
- [37] Lin Xu, Yilin Zhao, Daquan Zhou, Zhijie Lin, See Kiong Ng, and Jiashi Feng. Pllava: Parameter-free llava extension from images to videos for video dense captioning. *arXiv preprint arXiv:2404.16994*, 2024. 2, 4
- [38] Hongwei Xue, Tiankai Hang, Yanhong Zeng, Yuchong Sun, Bei Liu, Huan Yang, Jianlong Fu, and Baining Guo. Advancing high-resolution video-language representation with large-scale video transcriptions. In *International Conference on Computer Vision and Pattern Recognition (CVPR)*, 2022. 7, 8
- [39] Zhou Yu, Dejing Xu, Jun Yu, Ting Yu, Zhou Zhao, Yueting Zhuang, and Dacheng Tao. Activitynet-qa: A dataset for understanding complex web videos via question answering. In *Proceedings of the AAAI Conference on Artificial Intelligence*, pages 9127–9134, 2019. 6
- [40] Xiaohua Zhai, Basil Mustafa, Alexander Kolesnikov, and Lucas Beyer. Sigmoid loss for language image pre-training. In *Proceedings of the IEEE/CVF International Conference on Computer Vision*, pages 11975–11986, 2023. 4, 7, 8
- [41] Hang Zhang, Xin Li, and Lidong Bing. Video-llama: An instruction-tuned audio-visual language model for video understanding. *arXiv preprint arXiv:2306.02858*, 2023. 6
- [42] Hang Zhang, Xin Li, and Lidong Bing. Video-llama: An instruction-tuned audio-visual language model for video understanding. *arXiv preprint arXiv:2306.02858*, 2023. 2
- [43] Yuanhan Zhang, Bo Li, haotian Liu, Yong jae Lee, Liangke Gui, Di Fu, Jiashi Feng, Ziwei Liu, and Chunyuan Li. Llava-next: A strong zero-shot video understanding model, 2024. 2
- [44] Yuanhan Zhang, Jinming Wu, Wei Li, Bo Li, Zejun Ma, Ziwei Liu, and Chunyuan Li. Video instruction tuning with synthetic data. *arXiv preprint arXiv:2410.02713*, 2024. 4
- [45] Zijia Zhao, Yuqi Huo, Tongtian Yue, Longteng Guo, Haoyu Lu, Bingning Wang, Weipeng Chen, and Jing Liu. Efficient motion-aware video mllm, 2025. 2
- [46] Chunting Zhou, Lili Yu, Arun Babu, Kushal Tirumala, Michihiro Yasunaga, Leonid Shamis, Jacob Kahn, Xuezhe Ma, Luke Zettlemoyer, and Omer Levy. Transfusion: Predict the next token and diffuse images with one multi-modal model. *arXiv preprint arXiv:2408.11039*, 2024. 3
- [47] Junjie Zhou, Yan Shu, Bo Zhao, Boya Wu, Shitao Xiao, Xi Yang, Yongping Xiong, Bo Zhang, Tiejun Huang, and Zheng Liu. Mlvu: A comprehensive benchmark for multi-task long video understanding. *arXiv preprint arXiv:2406.04264*, 2024. 6

Appendix

A. Details of ELVA Model

A.1. Training Details

Tab 7 summarizes the hyperparameters used across different training stages. During the spatial pretraining stage, we adopt a low number of frames, increasing to 32 frames for both the spatial-temporal pretraining and supervised fine-tuning (SFT) stages.

Table 7. **Hyper-parameter Settings for Training Details.** PE denotes Patch Embedding, TC represents the Temporal-Capture Block, TH refers to the Task Head, and LM indicates the language model.

Hyperparameter	Stage 1	Stage 2	Stage 3
Data Scale	1M	7M	843K / 3M
Batch Size	256	256	128 / 256
Video Frame	1	16	32
Hierarchical Merge	✗	✗	✓
Learning Rate (lr)	4e-5	4e-5	2e-5
LR Schedule	cosine decay	cosine decay	cosine decay
LR Warmup Ratio	0.03	0.01	0.01
Epoch	1	2	1
Weight Decay		0	
Optimizer		AdamW	
DeepSpeed stage		2	

We utilize a total of 4M image samples, comprising 1M from Densefusion and 3M from re-annotated CC3M and COCO in stage 1. For stage 2, we employ 3M re-annotated samples, including 2M from WebVid [3] and 1M from VALOR [5]. See Table 8 for a detailed breakdown of data sources.

A.2. Prompt Engineering

We utilize the following prompt in table 9 to generate detailed captions for the provided images and videos using Qwen2-VL (7B) [33]. For image data, we limit the maximum pixel count to $1280 \times 28 \times 28$ to ensure computational efficiency. Using 16 Nvidia A100 GPUs, generating 3 million high-quality image descriptions takes approximately two days. For video data, we process frames at a rate of 1 fps, with the maximum pixel count per frame set to 360×420 . Generating 3 million video captions under these settings requires three days with 16 Nvidia A100 GPUs.

B. Evaluations on Image-Language Benchmarks.

Evaluation on Image-Language Benchmarks. We evaluate ELVA on a series of general visual understanding benchmarks including GQA [14], SEED-Bench [17], MME [12], MMBench [24]. Part of the image results of Chameleon

Table 8. Data used in pre-training and multimodal supervised fine-tuning stages. * indicates the data is used only in ELVA-7B (HD).

Stage	Dataset	Scale	Source
Stage 1	ELVA-Image	3M	CC-3M, COCO
	DenseFusion	1M	LAION-2B
Stage 2	ELVA-Video	3M	Webvid-2.5M, VALOR-1M
	LLaVA-Video	178K	NeXT-QA, ActivityNetQA, PerceptionTest, LLaVA-Hound
Stage 3	LLaVA-665K /	665K /	COCO, VG, OCR-VQA, GQA, TextVQA
	LLaVA-One Vision*	3M*	High-Quality Single-Image

Image Prompt	Video Prompt
<p>You are a powerful multimodal model and you should generate detailed descriptions of this image, including information such as [World Knowledge], [Objects], and [OCR]. Although the information may contain errors or be incomplete, you should disregard any inaccuracies. If any information is not used, do not specify why.</p> <p>[Additional Information]:</p> <ul style="list-style-type: none"> • [World Knowledge]: {SHORT CAPTION} • [Objects]: <ul style="list-style-type: none"> - {OBJECT AA} - {OBJECT BB} - ... • [OCR]: <ul style="list-style-type: none"> - {SENTENCE A} - {SENTENCE B} - ... <p>[IMAGE]:</p>	<p>You are a powerful multimodal expert in understanding scene transitions based on visual features in a video. You are requested to create the descriptions for the current clip sent to you, which includes multiple sequential frames.</p> <p>[Guidelines For Clip Description]:</p> <ul style="list-style-type: none"> • Analyze the narrative progression implied by the sequence of frames, interpreting the sequence as a whole. • Note that since these frames are extracted from a clip, adjacent frames may show minimal differences. These should not be interpreted as special effects in the clip. • When referring to people, use their characteristics, such as clothing, to distinguish different people. • **IMPORTANT** Please provide as many details as possible in your description, including colors, shapes, and textures of objects, actions and characteristics of humans, as well as scenes and backgrounds. <p>[VIDEO]:</p>

Table 9. **Prompt for Caption Engine.**

Table 10. **Evaluation on image-language benchmarks.** Our evaluation involves GQA, MME, MM Bench (MMB), and SEED. The results in **bold** and underline are the best and second-best results among encoder-free models, respectively.

Model	Data	GQA	SEED ₁	MME	MMB
<i>Encoder-based Models</i>					
Qwen-VL [2]	7.2B	57.5	58.2	1487.5	60.6
LLaVA-v1.5 [23]	0.4B+	62.0	58.6	1510.7	64.3
LLaVA-1.6 (HD) [23]	0.4B+	64.2	64.7	1519.3	67.4
<i>Encoder-free Models</i>					
Fuyu-8B [4]	-	-	-	-	10.7
Chameleon [31]	1.4B+	-	30.6	170	31.1
EVE [10]	33M	60.8	61.3	1217.3	49.5
SOLO [7]	43.7M	-	64.4	1260	-
EVE (HD) [10]	33M	62.6	64.6	1305.7	52.3
ELVA	7M	<u>60.5</u>	<u>66.5</u>	1262.1	<u>53.8</u>
ELVA (HD)	7M	<u>61.1</u>	67.2	<u>1291.5</u>	58.2

and EVE are evaluated with VLMEvalKit [11] or from the OpenCompass.

B.1. Visualization on Data

We provide additional examples from the ELVA datasets in Table 11. For enhanced visualization, different colors are used to highlight distinct types of information within the descriptions.

Table 11. Visualizations of the descriptions in ELVA-Image and ELVA-Video. For enhanced clarity, information related to *objects/attributes*, *spatial positions/scene changes*, and *text information* is highlighted using distinct colors.

Visualization	Detailed Caption
	<p>The image depicts a red and black train, stationed at a platform. The train is numbered 96104 and is positioned on the tracks, ready to depart or having just arrived. The platform is equipped with a yellow safety line and a metal fence on the right side. In the background, there is a pedestrian bridge and some buildings, indicating an urban setting. The weather appears to be clear, and the overall scene is well-lit.</p>
	<p>The image depicts a cozy living room with a modern and somewhat industrial aesthetic. The room features two black leather sofas, one of which is positioned against the wall and the other facing the television. The sofas are arranged around a wooden coffee table, which has a few items on it, including a small plant and a cup. ... On the right side of the room, there is a flat-screen television mounted on the wall. Below the television, there is a small shelf with a few items on it. In the background, there is a poster on the wall with the text "ROXY PRO FIJI" visible, suggesting a connection to surfing or a surfing event. The room also contains a guitar leaning against the wall, adding a personal touch to the space.</p>
	<p>The video begins with a title screen that reads "A LIFESTYLE." The scene then shifts to a man wearing a white t-shirt, black cap, and sunglasses, standing in front of a car at night. The man appears to be talking or speaking, and the background shows a brightly lit gas station with an American flag and a sign that reads "2 for \$2.22." The scene suggests a casual, relaxed atmosphere, possibly indicating a lifestyle that involves leisure activities and spending time outdoors.</p>
	<p>The video opens with a close-up shot of a white fireplace with a warm fire burning inside. The flames flicker and dance, casting a cozy glow on the surrounding area. As the camera pans out, we see that the fireplace is situated in a well-decorated room, with a potted plant and a few decorative items placed on the mantel. The walls are painted a warm beige color, and the floor is covered with a soft, plush carpet. The overall atmosphere is one of warmth and comfort, with the fire providing a focal point for the room.</p>